Chemically Mediated Quantum Criticality in NbFe_{2}

Aftab Alam and D. D. Johnson

Chemically-Mediated Quantum Criticality in NbFe$_2$

Aftab Alam[1] and D. D. Johnson[1,2*]

[1]*Division of Materials Science and Engineering, Ames Laboratory, Ames, Iowa 50011; and*

[2]*Department of Materials Science & Engineering, Iowa State University, Ames, Iowa 50011.*

Laves-phase Nb$_{1+c}$Fe$_{2-c}$ is a rare itinerant intermetallic compound exhibiting magnetic quantum criticality at $c_{cr} \sim 1.5\%$Nb excess; its origin, and how alloying mediates it, remains an enigma. For NbFe$_2$, we show that an unconventional band critical point (uBCP) above the Fermi level E$_F$ explains most observations, and that chemical alloying mediates access to this uBCP by an increase in E$_F$ with decreasing electrons (increasing %Nb), counter to rigid-band concepts. We calculate that E$_F$ enters the uBCP region for $c_{cr} > 1.5\%$Nb and by 1.74%Nb there is no Nb site-occupation preference between symmetry-distinct Fe sites, i.e., no electron-hopping disorder, making resistivity near constant as observed. At larger Nb (Fe) excess, the ferromagnetic Stoner criterion is satisfied.

PACS numbers: 71.20.Lp,75.10.Lp,75.45.+j

Quantum criticality emerges from collective low-energy excitations leading to a second-order phase transition at zero temperature (T).[1] In the study of correlated-electron materials, e.g., high-T superconductors and heavy-Fermion compounds, understanding such critical phenomenon remains a principal challenge; and, locating any existing quantum critical points (QCPs) is difficult. Near these QCPs, quantum fluctuations (rather than thermal fluctuations) are observed to give rise to exotic effects, e.g., non-Fermi liquid behavior.[2] In intermetallic compounds the situation appears simpler, where, by varying non-thermal order parameters, such as applied pressure, external magnetic field, or chemical doping, various phases near a QCP can be accessed, i.e., ferromagnetic (FM), antiferromagnetic (AFM), and paramagnetic (PM) states. Importantly, strong electron-electron interactions are not required for an alloy to show correlated behavior, as now confirmed in Fe-As compounds.[3] The Laves phase of Nb$_{1+c}$Fe$_{2-c}$ is one important example and featured in recent reviews of quantum criticality in weak magnets.[4] At stoichiometry the susceptibility exhibits Curie-Weiss behavior down to a spin-density wave (SDW) transition at T$_{sdw} \simeq 10$ K, whereas at $\sim 1.5\%$Nb excess a QCP is observed where the SDW collapses and non-Fermi-liquid behavior occurs.[5,6] For larger Nb *excess* ($c > 0$, hole doping) or Fe *excess* ($c < 0$, electron doping) a FM transition is always observed.[5,6] Indeed, the sensitivity of the magnetic state to Nb deficiency has long been known.[7,8]

Although well characterized experimentally, our understanding of the properties of Nb$_{1+c}$Fe$_{2-c}$ is lacking, especially how chemical disorder affects the magnetic transitions and QCP, and the FM onset at larger dopings. Recent theoretical work studied the electronic properties of NbFe$_2$,[9] but did not address the critical chemical effects. Of course, including properly the effects of disorder in these class of systems, specifically at such a small doping (c), is a considerable challenge. Attempting to address doping, recent studies use the virtual crystal approximation[10] (VCA) or supercells (ordered array of

dopants),[11] having severe shortcomings, as we discuss.

In metals low-energy excitations lie at/near the Fermi surface (FS), and, thus, some unique spectral feature at/near E$_F$ is typically required to drive a transition, as with FS nesting[12,13] or van Hove band critical points[14] (BCP) types of ordering.[15,16] Such FS features have been rarely identified as the origin of quantum criticality. We detail how an unconventional BCP (uBCP), i.e., an accidental saddle-point dispersion, above E$_F$ is responsible for the QC behavior in metallic Nb$_{1+c}$Fe$_{2-c}$. We show that chemical disorder mediates, via d-state hybridization, access to this uBCP even with fewer electrons for increasing %Nb, which rigid-band/VCA cannot describe, effects well known in alloy theory.

We use an all-electron, Korringa-Kohn-Rostoker (Green's function) electronic-structure method and the Coherent-Potential Approximation[17] (KKR-CPA) to calculate the electronic dispersion, density of states, total energies and doping site-preferences in Nb$_{1+c}$Fe$_{2-c}$. See Ref. 18 for details and examples for (dis)ordered alloys. In agreement with experiment, we calculated c_{cr} "onset" at 1.5%Nb, and, at 1.74%Nb, when E$_F$ lies exactly at the uBCP, we find that Nb has no site-occupation preference between the two symmetry-distinct Fe sites, favoring a homogeneous solute distribution and no electron-hopping disorder, suggesting a near constant resistivity. We find competing FM and AFM states, as observed, that are associated with the competing wavevectors from the uBCP. We show that the FM Stoner criterion in Nb$_{1+c}$Fe$_{2-c}$ is obeyed for larger Nb (or Fe) excess. If the uBCP are removed from consideration, none of these results hold. We conclude that the QCP occurs via chemical-disorder-mediated access to the uBCP above E$_F$.

To understand chemical disorder effects, we first need to appreciate the structure of NbFe$_2$, which crystallizes in a C14 hexagonal Laves phase with space group P6$_3$/mmc (#194). In terms of crystallography, NbFe$_2$ $\equiv$ Nb$_4$Fe$_2^{(2a)}$Fe$_6^{(6h)}$ with a 12-atom unit cell: Fe$^{(6h)}$ sites form two Kagome networks ($\perp$ to c-axis) separated by Fe$^{(2a)}$ sites in a hexagonal sublattice, and Nb atoms oc-
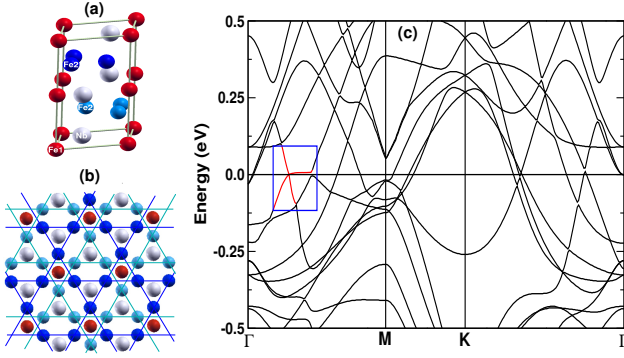
FIG. 1. (Color online) (a) Laves unit cell. (b) $Fe^{(6h)}$ sites form two Kagome nets, with Nb (gray), $Fe^{(2a)}$ (red) and $Fe^{(6h)}$ (blue), with higher (lower) planes shaded. (c) $NbFe_2$ bands (E_F at 0 eV). Highlighted box shows an uBCP above E_F.

FIG. 2. (Color online) (a) $\Delta E_F(c)$ shift due to %Nb-excess vs. e/a for $Nb_4(Fe_{1-c}Nb_c)_8$. E_F lies at uBCPs at $c_{cr} = 1.74\%$ but enters spectral tails at 1.65%. Inset (a) shows (un)doped $A_B^{max}(\mathbf{k}; E)$ along Γ-M, and (b) expands around uBCPs (bars are spectral widths due to disorder broadening).

cupy the interstices, see Fig. 1(a,b). The Wykoff positions (without inversion) are: Nb at $4f(\frac{1}{3}, \frac{2}{3}, x)$, $Fe^{(2a)}$ at $2a(0, 0, 0)$ and $Fe^{(6h)}$ at $6h(y, 2y, \frac{3}{4})$. Calculations are performed with measured[5] structural parameters $a = 4.8401$ Å, $c = 7.8963$ Å and internal coordinates $x = 0.0629$ and $y = 0.1697$. Using KKR-CPA we may study the effect of (in)homogeneous solute distributions. Disorder with antisite Nb on one or both Fe sublattices is written as $Nb_4(Fe_{1-c^{(2a)}}^{(2a)} Nb_{c^{(2a)}}^{(2a)})_2 (Fe_{1-c^{(6h)}}^{(6h)} Nb_{c^{(6h)}}^{(6h)})_6$, or $Nb_4(Fe_{1-c}Nb_c)_8$ for the homogeneous case.

To identify critical electronic features and chemical disorder effects, we detail the dispersion $\epsilon(\mathbf{k}; E)$ and density of states (DOS). KKR uses constant-E matrix inversion to get $\epsilon(\{\mathbf{k}\}; E)$, rather than constant-$\mathbf{k}$ diagonalization to get eigenvalues $\epsilon(\mathbf{k}; \{E\})$. To handle (dis)ordered cases, we calculate the Bloch spectral function[13] $A_B(\mathbf{k}; E)$ on a grid of $32 \times 32 \times 24$ $\mathbf{k}$-points to project the dispersion. For ordered cases, $A_B(\mathbf{k}; E)$ yields $\delta(E - \epsilon(\mathbf{k}; E))$, i.e., bands; otherwise it exhibits disorder-induced spectral broadening in E and $\mathbf{k}$, related to the finite electron scattering length.

We now show that the c-dependence tied to the observed quantum criticality arises from the $NbFe_2$ dispersion above E_F. Our bands in Fig. 1(c) agree with those from full-potential methods.[9] The bands crossing E_F along Γ-M arise mainly from $Fe^{(6h)}$ t_{2g}-orbitals, and lead to *saddle-point dispersion* slightly (6.6 meV) above E_F with an unusual flat dispersive region (uBCP), Figs. 1(c) and 2(b). These uBCP near E_F are not a result of symmetry, but arise from accidental band crossings. Experimentally, Crook and Cywinski[19] inferred that the $Fe^{(6h)}$ t_{2g}-orbitals in the Kagome nets plays a critical role in the competing magnetic order associated with the quantum phase transition (QPT). The $Nb_{1+c}Fe_{2-c}$ phase diagram[5] shows the QCP onset at ambient pressure at $c_{cr} \sim 1.5\%$Nb (hole-doped) and extends to $c \simeq 2.0\%$, with FM at larger doping. For a metal, only low-energy excitations near E_F can be relevant for such low-T transitions. By small tuning of a non-thermal order parameter,
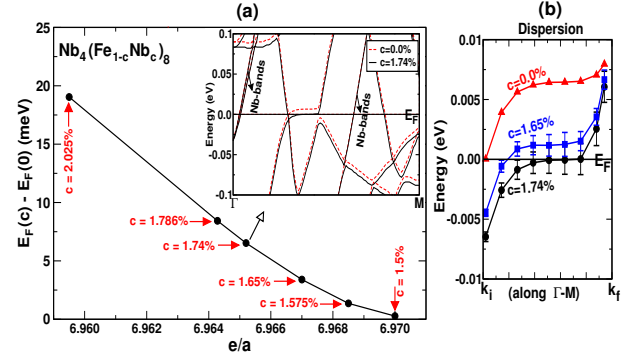
i.e., c, the unusual QPT behavior is observed, and can be explained if these uBCPs are accessed.

For homogeneous doping, we find a chemical-disorder-mediated increase of $E_F(c)$ versus %Nb excess, or decreasing electron-per-atom (e/a) ratio, Fig. 2(a). Counter to rigid-band concepts, E_F rises to uBCP and due to Fe-Nb (*bond/antibond*) alloying hybridization in Kagome nets Fe-bands shift lower but bands from the pure Nb-layer remain unaffected, Fig. 2(a) inset. (An ordered array of impurities exaggerates the effect, see below, showing disorder plays a key role.) At 1.74%Nb excess, uBCP lay at E_F, a 6.6 meV shift due to alloying and disorder (finite life-time) effects, see Fig. 2(b). The 6.6 meV (or 77 K) sets the maximum temperature, as observed, for these effects to occur on stoichiometry. The dispersion and disorder-induced widths along $\Gamma-M$ for $0 \le c \le c_{cr}^{cpa}$, Fig. 2(b), estimates the QC range. By 1.65%, E_F enters the spectral tails, giving zero-energy excitations into the anomalous dispersion; E_F is maximally aligned with the uBCP by 1.74% (giving a Lifshitz-type transition, see below), and exits by 2%, where FM is observed. We conclude that the QCP occurs from alloying/disorder-mediated access to the uBCP inherent in $NbFe_2$ dispersion above E_F, detailed more below.

We have performed supercell calculations to illustrate how sensitive $\Delta E_F(c)$ is to approximations used to address chemical effects, which ignore disorder. Supercells are numerically costly due to large cells needed with decreasing %Nb. We performed calculations at two concentrations with cells constructed by substituting a Nb-atom for one Fe-atom in a $2 \times 2 \times 1$ (6.25%Nb excess) and a $2 \times 2 \times 2$ (3.125%Nb excess) supercell. The supercells also yield a $\Delta E_F(c)$ increase, relative to $c = 0\%$, of 117.1 and 281.3 meV for 3.125% and 6.25%Nb excess, respectively. The CPA shifts are 65.4 and 158.1 meV, respectively, which lie on the curve in Fig. 2(a) at smaller e/a. So, supercells do not provide the correct occupancy probability nor hybridization across the Kagome net, missing the key disorder effects. Nonetheless, supercell results
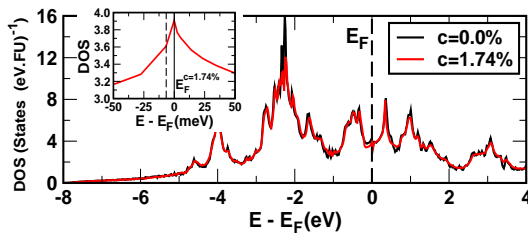
FIG. 3. (Color online) Non-magnetic DOS per formula unit relative to E_F for $Nb_{1+c}Fe_{2-c}$ at $c_{cr} = 0$ and 1.74%. Inset: DOS at c_{cr} around E_F (vertical dashed line is E_F at c=0%).

do reinforce the fact that rigid-band/VCA concepts are invalid, missing the critical alloying and disorder effects.

Figure 3 compares the DOS for $Nb_{1+c}Fe_{2-c}$ at c_{cr} to 0%, which is similar to full-potential results.[9,11] Disorder broadening for $c > 0$% is evident. E_F lies near a precipice of a DOS depression, which plays a role in forming a SDW state at $c = 0$. $n(E_F)$ is 3.59 states (eV - formula unit)$^{-1}$ for $NbFe_2$. Notably, for $NbFe_2$, unlike conventional BCP,[14] the *saddle-point dispersion* at $\mathbf{k}$'s associated with the uBCP is (beyond) cubic ($\epsilon_k \propto k_x^3$) in one direction and quadratic in the orthogonal k_y, k_z plane, yielding an chemically-mediated peak in $n(E_F)$ when E_F and uBCP are aligned, Fig. 3 inset. From Stoner theory with interaction parameter I,[20] a FM instability occurs if $n(E_F)I > 1$. For pure Fe d-electrons, I was reported[21] between $0.7 - 0.9$ eV. From susceptibility data for $NbFe_2$, the Stoner factor $[1 - n(E_F)I]^{-1}$ was estimated[5] at ~ 100. Our calculated I for $Nb_{1+c}Fe_{2-c}$ is almost constant versus c ($0.88 \le I \le 0.9$), but $n(E_F)$ increases with doping, increasing $n(E_F)I$, e.g., $n(E_F)$ for 1.74%Nb increases to 3.90 states-(eV FU)$^{-1}$. Stoner's criterion is satisfied beyond 2%Nb, as observed, and discussed more below.

Lifshitz transitions are mediated by FS topology changes (e.g., collapse of FS neck or loss of pockets). An unconventional Lifshitz transition emerging near a *marginal* QCP was proposed in $ZrZn_2$.[22] Such a zero-temperature, pressure-induced transition is also associated with access to an uBCP by an increase in E_F. The FS topology changes are reflected in a maximum in $n(E_F)$ at the Lifshitz point, as we found for hole-doping in $NbFe_2$ at $c_{cr} = 1.74$% (Fig. 3 inset). Not only the topology, but the FS volume is strongly dependent on doping, and in $NbFe_2$ enhanced with hole doping, and also observed in a hole-doped $Ba_{0.3}K_{0.7}Fe_2As_2$.[23]

To explore beyond the QCP, we studied doping in the Fe- and Nb-rich parts of the phase diagram. The DOS (atom- and impurity-projected) for 3.125% Nb- and Fe-rich $Nb_{1+c}Fe_{2-c}$ is shown in Fig. 4. The Nb-rich (hole-doped) $n(E_F)$ increases to 4.66 states-(eV FU)$^{-1}$. Fe-rich (electron-doped) alloys behave opposite to what is expected from rigid-band theory; i.e. with electron doping, $n(E_F)$ rises to 4.75 states-(eV FU)$^{-1}$, which is mainly due to Fe-impurity DOS originating from Nb-layers, see Fig. 4 (lower panel). These values of Nb-rich and Fe-rich $n(E_F)$ satisfy the FM Stoner criterion, as observed.[5]

We have also studied how the nature of the uBCP (or QCP) is affected by inhomogeneous Nb doping on the two Fe sublattices. We find that, if only $Fe^{(6h)}$ sites are doped, the uBCP lies at E_F when $c_{cr}^{(6h)} = 2.34$%, for an average $c_{cr}^{avg} = 2.34\% \times (6/8) = 1.75$%. For $Fe^{(6h)}$-only case, dispersion is similar to the homogeneous case as in Fig. 1(c), because mainly $Fe^{(6h)}$ t_{2g}-orbitals within the Kagome sheets are involved. In contrast, if only $Fe^{(2a)}$-sites are doped, the uBCP lies at E_F when $c_{cr}^{(2a)} = 8.7$%, i.e., $c_{cr}^{avg} = 8.7\% \times (2/8) = 2.02$%. The shift of E_F relative to dispersion in this case arises due to hybridization of $Fe^{(2a)}$-states indirectly with $Fe^{(6h)}$-states. Dispersion with $Fe^{(2a)}$-only doping shows an increased slope of the uBCP compared to the other cases, changing the character and c-dependence of the response.

In Fig. 5 we report Nb site-preference energy differences $(E^{(6h)} - E^{(2a)})$ versus %Nb-excess in $Nb_4(Fe_{1-c^{(2a)}}^{(2a)}Nb_{c^{(2a)}}^{(2a)})_2(Fe_{1-c^{(6h)}}^{(6h)}Nb_{c^{(6h)}}^{(6h)})_6$, where $E^{(\alpha)}$ is the total energy when only the $Fe^{(\alpha)}$-sites are doped. At $c_{cr}^{cpa} = 1.74$%, where the uBCP lies at E_F, there is no energetically favored site occupancy, therefore, no electron-hopping disorder effects, explaining the observed extremely slow variation of ρ versus doping.[5] With no site preference, a homogeneous solute distribution is favored, further supporting our focus on this case. These results shed light on the microscopic phenomenon occurring at/near the QCP: the alignment of E_F with the uBCP at 1.74% provides maximum response concomitant with no electron-hopping disorder and instability to both AFM and FM fluctuations.

We now explore the stability of competing magnetic phases. Out of several small-cell, magnetic configurations in $NbFe_2$, we found a AFM state energetically favored by -10.45 meV/atom over the non-magnetic state, where local moments on the $Fe^{(2a)}$- and $Fe^{(6h)}$-sites are aligned antiparallel with values of 0.69 μB and -0.98 μB, respectively, and the Nb has an induced moment of 0.14 μB aligned with the $Fe^{(2a)}$-site. The same ground state was found in other calculations.[9,11] The phase diagram indi-
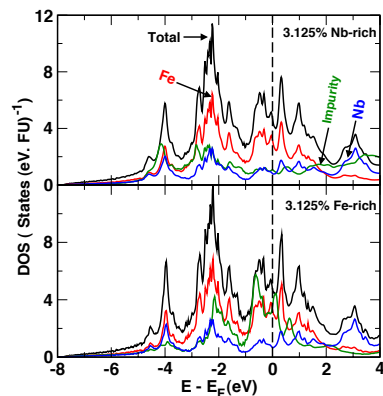

FIG. 4. (Color online) Non-magnetic DOS relative to E_F for 3.125% Nb-rich (top) and 3.125% Fe-rich (bottom).
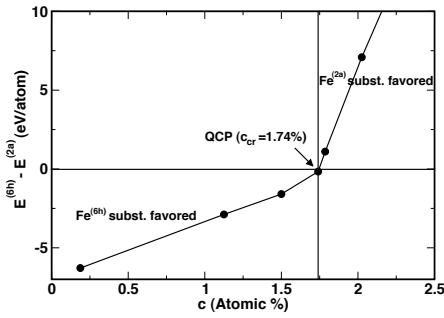
4

FIG. 5. Nb site-preference energy difference $(E^{(6h)}-E^{(2a)})$ versus %Nb excess in $Nb_4(Fe_{1-c}Nb_c)_8$. $E^{(\alpha)}$ is the total energy when only the $Fe^{(\alpha)}$-sites are doped. At $c_{cr} = 1.74\%$, no Fe-site is favored, i.e., homogeneous solute distribution.

cates a SDW state for $NbFe_2$ with a highly itinerant nature (as for iron-arsenides[3]), which competes with nearby FM states. The itineracy of magnetism is clear from the spin density on Fe-sites, see Supplement, while carrier density peaks at c_{cr}, Fig. 3 inset.

To connect to scattering experiments, the uBCP $\epsilon(\mathbf{k})$ exhibit zero-velocity quasiparticles near E_F at symmetry-equivalent, non-special $\mathbf{k}$-points $Q_0(\pm 1, 0)$ and $Q_0(\pm\frac{1}{2}, \pm\frac{\sqrt{3}}{2})$, where $Q_0 \approx 0.25$ in units of the $\Gamma-M$ caliper in Fig. 1(c). These Q's remain relevant for off-stoichiometric alloys. The susceptibility, i.e.,

$$\chi(\mathbf{q}) = \sum_{\mathbf{k}}[f(\epsilon_{\mathbf{k}}) - f(\epsilon_{\mathbf{k+q}})][\epsilon_{\mathbf{k+q}} - \epsilon_{\mathbf{k}}]^{-1} \ , \qquad (1)$$

can exhibit an enhanced response due to a convolution of (un)occupied states near E_F, as for FS nesting.[12,13] Albeit weaker, it can occur from saddle-point topology too. From the small caliper of the flat part of the uBCP, i.e., $0.055(2\pi/a)$, we estimate a $|q|$ of $0.07 \mathring{A}^{-1}$ close to the $0.05 \mathring{A}^{-1}$ estimated from experiment.[6]

Thus, from our direct calculations or estimated $\chi(\mathbf{q})$ features, PM, FM and SDW (AFM) states compete near the QCP, until overwhelmed by a Stoner instability at larger $|c|$, shown above. Such competing magnetic behavior is observed[6] near the QCP, where the low-T resistivity $(\rho(T) \sim T^\nu)$ exponent ν varies between 3/2 and 5/3, giving unusual non-Fermi liquid behavior.

Quantifying the anomalous response further requires $\chi(\mathbf{q}, c, \omega)$, which is beyond the present scope. But, the change in $\omega=0$ susceptibility, $\Delta\chi(Q, \omega=0)$, yields the change in the DOS at E_F, i.e., $\Delta n(E_F)$, and, if large, a FM instability. Neal et al. have extended the Moriya $\chi(\mathbf{q}, c=0, \omega)$ theory to account for uBCP, which yields an anomalous frequency response and competing FM and SDW states,[24] agreeing with our direct calculations.

In summary, we have identified an accidental Fermi-surface (non-ideal saddle-point) dispersion as the origin for observed behavior associated with the quantum criticality in $Nb_{1+c}Fe_{2-c}$. We find that Nb (hole) doping accesses an unconventional band critical points in $NbFe_2$ that provide the necessary low-energy excitations for a (Lifshitz-type) transitions. This origin explains most of the observed doping behavior in this QC intermetallic compound, specifically, (i) onset of c_{cr} %Nb-excess for the QCP; (ii) almost constant resistivity versus c, (iii) competing magnetic states and temperature scale, (iv) observed SDW wavevectors, and, finally, (v) the stable FM states at large hole- or electron-doping (>2%). To explore the nature of the QC transition further, these electronic and chemical features can be incorporated into a model Hamiltonian, but they would not have been discovered without the full dispersion and chemical alloying effects detailed here.

Work funded by the U.S. Department of Energy BES-DMSE (DE-FG02-03ER46026) and Ames Laboratory (DE-AC02-07CH11358), operated by Iowa State University. We thank to W. Pickett for suggesting this problem.

* emails: ddj@ameslab.gov,aftab@ameslab.gov
[1] S. Sachdev, Science **288**, 475 (2000).
[2] H.v. Löhneysen et al., Rev. Mod. Phys. **79**, 1015 (2007).
[3] D. K. Pratt et al., Phys. Rev. Lett. **106**, 257001 (2011).
[4] A. J. Schofield, Phys. Stat. Sol. B **247**, 563 (2010); W. J., Duncan et al., Phys. Stat. Sol. B **247**, 544 (2010).
[5] M. Brando et al., Phys. Rev. Lett. **101**, 026401 (2008).
[6] D. Moroni-Klementowicz et al., Phys. Rev. B **79**, 224410 (2009).
[7] M. Shiga and Y. Nakamura, J. Phys. Soc. Jp. **56**, 4040 (1987).
[8] Y. Yamada and A. Sakata, J. Phys. Soc. Jpn. **57**, 46 (1988).
[9] A. Subedi and D. J. Singh, Phys. Rev. B **81**, 024422 (2010).
[10] D. J. Singh, Phys. Rev. B **78**, 094511 (2008).
[11] D. A. Tompsett, R. J. Needs, F.M. Grosche, and G.G. Lonzarich, Phys. Rev. B **82**, 155137 (2010).
[12] S. C. Moss, Phys. Rev. Lett. **22**, 1108 (1969).

[13] B. L. Györffy and G. M. Stocks, Phys. Rev. Lett. **50**, 374 (1983).
[14] L. van Hove, Phys. Rev. **89**, 1189 (1953).
[15] J. F. Clark et al., Phys. Rev. Lett. **74**, 3225 (1995).
[16] J. D. Althoff et al., Phys. Rev. Lett. **74**, 138 (1995).
[17] D. D. Johnson et al., Phys. Rev. Lett. **56**, 2088 (1986); Phys. Rev. B **41**, 9701 (1990).
[18] Aftab Alam and D. D. Johnson, Phys. Rev. B **80**, 125123 (2009); Aftab Alam, Brent Kraczek, and D. D. Johnson, Phys. Rev. B **82**, 024435 (2010).
[19] M. R. Crook and R. Cywinski, Hyperfine Inter. **85**, 203 (1994).
[20] E. Stoner, Proc. R. Soc. London, Ser. A **169**, 0339 (1939).
[21] O. K. Andersen et al., Physica B & C **86-88**, 249 (1977).
[22] Masatoshi Imada et al., J. Phys.: Condens. Matter **22**, 164206 (2010); Y. Yamaji et al., J. Phys. Soc. of Japan **76**, 063702 (2007).
[23] K. Nakayama et al., Phys. Rev. B **83**, 020501(R) (2011).

[24] Brian Neal *et al.*, Phys. Rev. B **84**, 085133 (2011).